Regular Article

PHYSICAL CHEMISTRY RESEARCH
Published by the
Iranian Chemical Society
www.physchemres.org
info@physchemres.org

Phys. Chem. Res., Vol. 14, No. 1, 209-226, March 2026
DOI: 10.22036/pcr.2026.536290.2757

Design and Computational Assessment of (1H-Pyrazolo[3,4-c] pyridin-5-yl) Sulfonamide Derivatives as Potent Hepatitis B Virus Capsid Assembly Modulators

A. Laoud[a,b,*] and A. Belafriekh[c]

[a]*Department of Chemical Engineering, Faculty of Chemical Engineering, University of Salah Boubnider Constantine 3, Constantine 25000, Algeria*

[b]*Laboratoire d'obtention de Substances Thérapeutique – LOST. Département de Chimie, Faculté des Sciences Exactes, Université Constantine 1, 25000, Algérie*

[c]*Laboratory of LCPMM, Organic Chemistry Department, Faculty of Sciences, University of Blida 1, P. O. Box: 270 Blida, 09000, Algeria*

(Received 27 September 2025, Accepted 30 January 2026)

Hepatitis B virus (HBV) is a significant global health concern, and the development of new antiviral agents is necessary. In this work, a comprehensive computational investigation was performed on a series of (1H-Pyrazolo[3,4-c] pyridin-5-yl) sulfonamide derivatives as potential antiviral agents to modulate HBV capsid assembly. Molecular docking studies were used to elucidate binding interactions with the HBV core protein, while atom-based 3D-QSAR modeling provided insights into key structural features governing antiviral activity. The developed 3D-QSAR model showed high statistical robustness and predictive power ($R^2 = 0.97$ for the training set, $Q^2 = 0.80$ for the test set, and RMSE = 0.17). Newly designed inhibitors, guided by contour map analysis and docking results, showed favorable binding affinity and ADME prediction, suggesting their potential as novel antiviral inhibitors.

Keywords: 3D-QSAR model, Hepatitis B virus, ADME prediction, Molecular docking

INTRODUCTION

Hepatitis B virus (HBV) infection remains a major global public health challenge, affecting an estimated 296 million individuals worldwide and resulting in approximately 820,000 deaths annually from associated liver diseases [1,2]. Chronic HBV infection is a significant risk factor for severe liver complications, including cirrhosis, liver failure, and hepatocellular carcinoma (HCC), which together contribute substantially to global morbidity and mortality. Despite the availability of effective vaccines and several antiviral therapies, the management of chronic HBV infection still faces significant obstacles [3]. Current standard of care treatments primarily includes nucleos(t)ide analogs and interferon-based therapies. While these agents efficiently inhibit HBV replication and reduce the viral load, they generally fail to achieve a complete functional cure [4]. This therapeutic limitation is largely attributed to the persistence of covalently closed circular DNA (cccDNA), a highly stable viral minichromosome maintained within the nuclei of infected hepatocytes [5]. The cccDNA serves as a continuous template for viral replication and transcription, maintaining its stability even under antiviral pressure, and poses a formidable obstacle to viral elimination [6,7]. Given these challenges, there is an urgent need to identify and develop novel antiviral agents that target alternative stages of the HBV life cycle beyond suppression of viral replication. Among emerging strategies, targeting the HBV core protein, a multifunctional structural protein, has gained significant attention [8]. The core protein plays an essential role in the viral life cycle by mediating nucleocapsid assembly, genome packaging, and facilitating reverse transcription of the viral pre-genomic RNA. Disruption of these processes *via* capsid assembly modulators (CAMs) has shown promise as a

*Corresponding author. E-mail: aicha.laoud@gmail.com

therapeutic approach to inhibit HBV replication and prevent viral propagation [9,10]. Among the various CAM scaffolds studied, compounds incorporating the sulfonamide moiety have demonstrated particular promise, frequently exhibiting high potency against the HBV core protein. In particular, the (1H-pyrazolo[3,4-c] pyridin-5-yl) sulfonamide derivatives have recently emerged as a highly effective and structurally distinct class of potent HBV capsid assembly inhibitors, warranting further structural investigation and optimization to improve their pharmacological profile [11]. In drug discovery efforts, computational methodologies have become indispensable tools to accelerate the identification and optimization of lead compounds [12,13]. Three-dimensional quantitative structure-activity relationship (3D-QSAR) modeling enables the correlation of molecular structural features with biological activity, providing valuable insights into ligand-receptor interactions and guiding rational drug design [14,15]. Complementary molecular docking approaches facilitate detailed characterization of ligand binding modes within target proteins, validating binding hypotheses and identifying key residues involved in interaction [16]. Furthermore, integrating such predictive models with in silico absorption, distribution, metabolism, and excretion (ADME) profiling enables early assessment of drug similarity and pharmacokinetic properties, simplifying the development of molecules with favorable efficacy and safety profiles [13,17]. In this work, we applied an integrated computational approach to study a dataset of 41 structurally diverse (1H-pyrazolo[3,4-c] pyridin-5-yl) sulfonamide derivatives previously reported as HBV capsid assembly modulators [11]. We developed a statistically robust atom-based 3D-QSAR model to elucidate the key structural determinants governing antiviral activity. Molecular docking analyses against the HBV core protein crystal structure (PDB ID: 5WRE) were performed to explore detailed binding interactions. Based on these insights, new compounds were designed and subjected to design and ADME profiling to evaluate their potential as effective and drug-like HBV capsid assembly inhibitors. This comprehensive approach aims to facilitate the rational design of next-generation antivirals with improved potency and pharmacokinetic profiles [18].

MATERIALS AND METHODS

Dataset Collection

For this study, a structurally diverse group of 41 (1H-Pyrazolo[3,4-c] pyridin-5-yl) sulfonamide derivatives was selected (Table 1) that have been reported in the literature as modulators of Hepatitis B Virus (HBV) capsid assembly [11]. With reported EC_{50} values ranging from 0.032 to 6 µM, these compounds exhibit a range of antiviral activity, indicating variable potency against HBV capsid formation [11]. The EC_{50} values were converted to their negative logarithmic form using the formula $pEC_{50} = -\log_{10}(EC_{50})$ to perform QSAR modeling [19].

Table 1. Experimental Data of Studied Compounds, Including Structure, EC_{50}, pEC_{50} (Experimental), pEC_{50} (Predicted), and Residual Values

Compd.	Structure	EC_{50} (µM)	PEC_{50exp}	PEC_{50pred}	Residual	Dataset
1	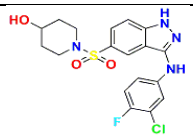	1.280	5.893	5.974	0.081	Training
2	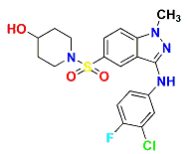	1.380	5.860	5.886	0.026	Training

Table 1. Continued

3	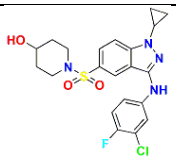	0.190	6.721	6.441	-0.280	Test
4	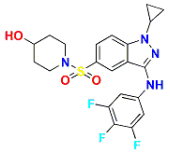	0.270	6.568	6.813	0.245	Training
5	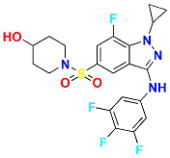	2.000	5.699	5.665	-0.033	Training
6	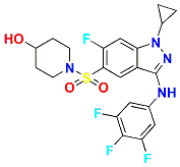	0.130	6.886	6.637	-0.249	Training
7	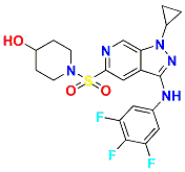	0.240	6.620	6.787	0.167	Training
8	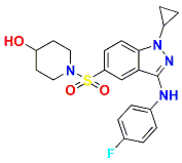	0.220	6.658	6.469	-0.189	Training
9	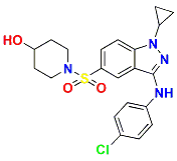	3.140	5.503	5.666	0.163	Training
10	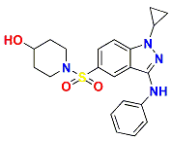	0.740	6.131	6.095	-0.036	Test
11	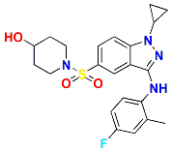	1.150	5.939	5.859	-0.080	Training

Table 1. Continued

12	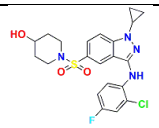	4.000	5.398	5.316	-0.082	Training
13	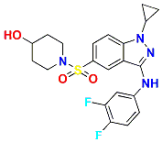	0.120	6.921	6.797	-0.124	Training
14	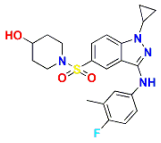	0.032	7.495	7.368	-0.127	Training
15	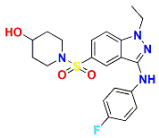	1.260	5.900	5.843	-0.057	Training
16		0.430	6.367	6.447	0.080	Training
17	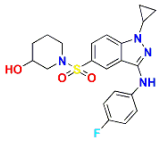	0.250	6.602	6.670	0.008	Training
18		2.100	5.678	5.824	0.146	Training
19	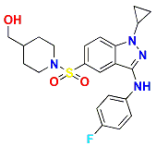	1.100	5.959	5.952	-0.007	Test
20	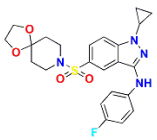	0.250	6.602	6.815	0.213	Training
21	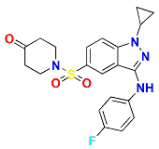	0.330	6.481	6.456	-0.025	Training

Table 1. Continued

22	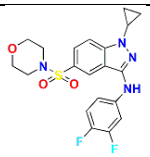	0.220	6.658	6.626	-0.032	Test
23	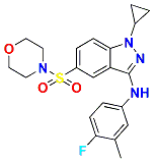	0.057	7.244	7.373	0.129	Training
24		0.210	6.678	6.969	0.291	Test
25		0.042	7.377	7.282	-0.095	Training
26	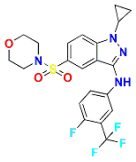	0.290	6.537	6.602	0.064	Training
27	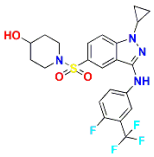	6.000	5.222	5.256	0.034	Training
28	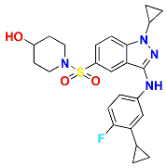	0.680	6.167	6.054	-0.113	Training
29	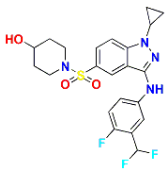	0.290	6.537	6.564	0.027	Training
30	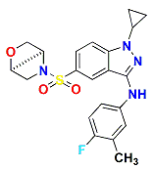	0.045	7.347	7.172	-0.175	Test

Table 1. Continued

31		0.120	6.921	6.751	-0.170	Training
32	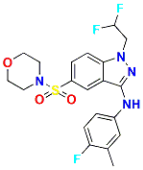	0.230	6.638	6.819	0.181	Test
33	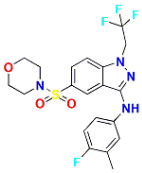	0.240	6.620	6.656	0.036	Training
34	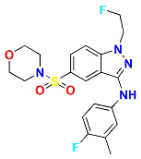	0.410	6.387	6.428	0.041	Training
35	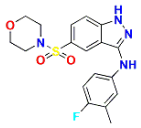	0.290	6.537	6.446	-0.091	Training
36		0.220	6.658	6.656	-0.002	Training
37		0.340	6.469	6.619	0.150	Test
38		0.230	6.638	6.641	0.003	Training
39	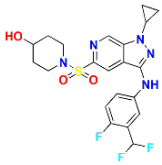	0.071	7.149	7.176	0.027	Training

Table 1. Continued

40	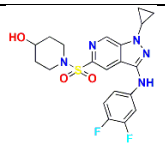	0.250	6.602	6.523	-0.079	Training
41	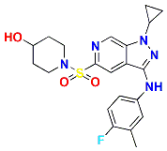	0.034	7.469	7.488	0.019	Training
GLS4	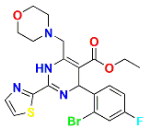	0.013	7.886	7.893	0.007	Training
AB-423	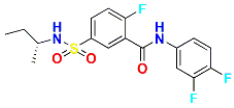	0.310	6.509	6.479	-0.030	Test

Ligand Preparation

The 2D chemical structures of 41 inhibitors and three reference molecules were initially drawn using the 2D sketcher module in Maestro. Subsequently, their 3D geometries were generated using the LigPrep module in Maestro [20]. The following parameters were applied during 3D structure preparation: (i) The OPLS-2005 force field was used for geometry optimization. (ii) For each molecule, one low-energy ring conformation was generated. (iii) All possible ionization states at physiological pH (7.0 ± 2.0) were considered. (iv) Where applicable, tautomers, chiral centers, and stereochemical variations were taken into account to ensure the generation of biologically relevant 3D conformations [21,22].

Molecular Docking

The crystal structure of the hepatitis B virus (HBV) core protein in complex with a heteroaryldihydropyrimidine ligand HAP-R01 (PDB ID: 5WRE, resolution: 1.95 Å) was retrieved from the RCSB Protein Data Bank (https://www.rcsb.org/structure/5WRE) [23]. Protein preparation was conducted using the Protein Preparation Wizard in Schrödinger, where all water molecules were removed, missing hydrogen atoms were added, and the protein structure was optimized and energy-minimized using the OPLS-2005 force field, with an RMSD convergence threshold of 0.30 Å [24]. A receptor grid was generated based on the co-crystallized ligand to define the binding pocket of the HBV core protein. All ligands were docked into this active site using Glide Extra Precision (XP) mode [25]. The docking protocol assessed binding poses and computed Glide docking scores to estimate ligand affinity and key interactions with active site residues [26].

Atom-based 3D-QSAR

An atom-based three-dimensional quantitative structure–activity relationship (3D-QSAR) study was performed using the PHASE module of Schrödinger [27,28]. The dataset comprising 41 compounds was randomly divided into a training set (80%) and a test set (20%) via the built-in random selection tool [29]. A grid spacing of 1 Å was applied to generate the atom-based descriptors. Partial Least Squares (PLS) regression was employed, with the number of PLS factors capped at N/5 (N = number of training compounds) to avoid overfitting. Based on this, four PLS factors were selected for the final QSAR model [30]. The model was validated by predicting biological activity (pEC_{50}) values of compounds in both the internal set and an external validation set, demonstrating robust predictive reliability [31].

Design of New Compounds

This study aims to propose new antiviral agents against the hepatitis B virus (HBV) and to support future drug development efforts. Guided by the molecular docking results, the interpretation of the results obtained from the 3D-QSAR model, as well as the structural features identified in the scaffold (Fig. 5), five new compounds (A1–A5) were designed as potential HBV inhibitors (Fig. 9). These compounds were docked into the binding site of the HBV core protein (PDB ID: 5WRE) using Glide XP to evaluate their binding affinities and interaction profiles. Finally, the five selected compounds were then submitted to PHASE to predict their antiviral activities using the developed atom-based 3D-QSAR model.

ADME Prediction

Compounds resulting from molecular docking were further evaluated for their pharmacokinetic profiles using the QikProp module of Schrödinger [32]. This ADME analysis provided essential physicochemical and pharmacokinetic parameters, including molecular weight (MW), solvent-accessible surface area (SASA), number of hydrogen bond donors (HBD) and acceptors (HBA), predicted aqueous solubility (QPlogS), lipophilicity (QPlogPo/w), cell permeability assessed by Caco-2 and MDCK models, brain-blood partition coefficient (QlogBB), skin permeability (QPlogKp), human oral absorption (HOA), and polar surface area (PSA). These parameters helped assess the drug-likeness and developability of the compounds [33].

RESULTS AND DISCUSSION

Atom-Based 3D-QSAR Model Analysis

A statistically robust and highly predictive atom-based 3D-QSAR model was developed for a series of 41 (1H-pyrazolo[3,4-c] pyridin-5-yl) sulfonamide derivatives to investigate the structural determinants of HBV capsid assembly inhibition. The optimal model was generated using four partial least squares (PLS) components, as summarized in Table 2. It demonstrated excellent statistical performance with a high regression coefficient (R^2 = 0.97 > 0.6) and a strong cross-validated determination coefficient (R^2_{cv} = 0.63 > 0.5), confirming good internal predictive ability for the training set. The low root-mean-square error (RMSE = 0.17) further demonstrates the accuracy and robustness of the model. External validation also confirmed strong predictive power, reflected in a high Q^2 value of 0.80 (Q^2 > 0.6) for the test set. Additional statistical parameters confirm the high level of confidence in the model: a large variance ratio (F = 209.3), a high Pearson-r of 0.90, and good overall model stability (0.72 on a scale of 1). Moreover, the extremely low P-value (6.11e-21) indicates the statistical significance of the regression. The small standard deviation (SD = 0.12) and low RMSE (0.17) confirm that the dataset used was optimal for QSAR analysis. The scatter plot of predicted versus experimental pEC_{50} values shown in Fig. 1 further confirms the excellent predictive performance and reliability of the 3D-QSAR model. Actual and predicted activities (pEC_{50}) and residual values of the dataset are presented in Table 1.

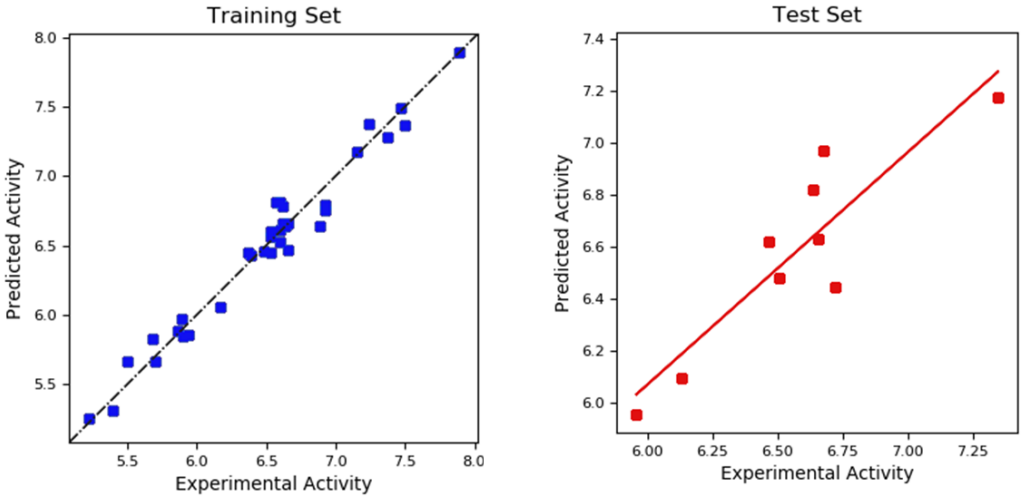

Fig. 1. Scatter plots of predicted *versus* experimental activity for the training set and the test set.

Table 2. Summary of 3D-QSAR PLS Statistical Parameters

Factors	SD	R^2	R^2_{CV}	R^2 $_{Scramble}$	Stability	F	P	RMSE	Q^2	Pearson-r
1	0.31	0.76	0.39	0.47	0.47	102.5	1.67e-11	0.19	0.74	0.88
2	0.21	0.89	0.57	0.74	0.77	127.4	1.11e-15	0.18	0.76	0.88
3	0.15	0.95	0.62	0.87	0.74	173.9	4.68e-19	0.17	0.78	0.88
4*	**0.12**	**0.97**	**0.63**	**0.93**	**0.72**	**209.3**	**6.11e-21**	**0.17**	**0.80**	**0.90**

*: Optimal model, SD: Standard Deviation (Smaller value), R^2: Regression coefficient ($R^2 > 0.6$), R^2_{cv}: Cross-Validated Correlation Coefficient ($R^2_{cv} > 0.5$), F: Ratio of the model variance (High value), P: Significance level of variance ratio (Smaller value), RMSE: Root-Mean-Square Error (Smaller value), Q^2: Correlation coefficient for the test set ($Q^2 > 0.6$), Pearson-r: Correlation between the predicted and observed activity.

Table 3. Field Contribution Summary of Atom-Based 3D-QSAR Model

PLS	H-Bond donor	Hydrophobic/non-polar	Electron-withdrawing	Other
1	0.048	0.543	0.341	0.069
2	0.054	0.544	0.351	0.052
3	0.058	0.570	0.328	0.044
4*	**0.062**	**0.575**	**0.332**	**0.041**

The field contribution analysis (Table 3) revealed that hydrophobic interactions are the dominant contributors to biological activity, contributing over 57% to the model. Electron-withdrawing features and hydrogen bond donor regions also played important supporting roles. Visual comparison between the most active compound (compound 14) and the least active compound (compound 27) confirmed these findings, highlighting favorable interaction zones around the core scaffold.

Contour maps Analysis

To better understand the structural factors governing the biological activity of the designed HBV capsid assembly modulators, atom-based 3D-QSAR contour maps were generated and analyzed for the most active compound (14, pEC_{50} = 0.032) and the least active compound (27, pEC_{50} = 6.000). These maps visually highlight favorable and unfavorable regions for various molecular properties, thus providing valuable guidance for rational structural modifications.

Hydrogen Bond Donor (HBD)

Figure 2 illustrates the hydrogen bond donor (HBD) contour maps for compounds 14 and 27. Blue cubes indicate regions where the presence of hydrogen bond donor groups significantly enhances biological activity, while red cubes indicate areas where donor groups reduce activity. In both compounds 14 and 27, favorable HBD regions are observed near the hydroxyl (-OH) group, and the blue cubes are also seen near the -NH group of the ligand. This suggests that these functional groups play a critical role in establishing strong interactions with the biological target, contributing significantly to the compound's activity.

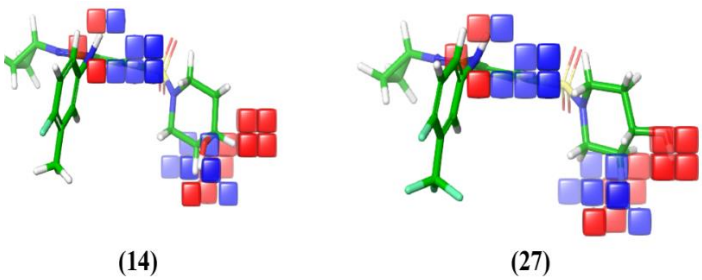

Fig. 2. Visualization of the hydrogen bond donor from the 3D-QSAR model on the most active compound (14) and the least active compound (27).

Hydrophobic Interaction

The hydrophobic interaction contour maps are shown in Fig. 3. Green cubes indicate regions where hydrophobic substituents positively influence biological activity. In compound 14, these favorable areas are observed near the 3-methyl group, the 4-fluoro group on the aniline ring, and the cyclopropyl group on the indazole scaffold. Similar favorable hydrophobic interactions are also observed in the pyrazolopyridine analogue compound 41 (pEC_{50} = 0.034), confirming that optimal placement of small hydrophobic groups significantly strengthens ligand-protein interactions. In contrast, the purple cubes indicate areas where hydrophobic substituents reduce activity. These unfavorable regions are observed near the position of the 3-trifluoromethyl (CF_3) group in compound 27. Because CF_3 is bulkier and sits in one of these unfavorable zones, it creates less optimal hydrophobic interactions, likely weakening binding compared to compound 14. Consequently, replacing the 3-methyl group with a 3-trifluoromethyl group significantly lowers the potency of these HBV capsid assembly modulators. Furthermore, the lower biological activity of compounds 1, 2, 3, 9, 11, and 12 can be explained by the absence of key hydrophobic elements such as the cyclopropyl group, the 3-methyl substituent, or the 4-fluoro group, which are essential for favorable hydrophobic interactions in the binding site. These contours provide strategic information to optimize hydrophobic interactions and thus improve the HBV capsid assembly modulator.

Electron-withdrawing

Figure 4 presents the electron-withdrawing contour maps derived from the 3D-QSAR model. Blue cubes represent areas where electron-withdrawing groups enhance biological activity, while yellow cubes indicate regions where these groups are detrimental to activity. For both compounds 14 and 27, blue cubes are located near sulfonamide ($–SO_2–N–R$) groups where electron-withdrawing substituents are present, suggesting that these groups contribute positively to their high activity. In contrast, the yellow cubes show regions where electron-withdrawing groups can impair biological activity.

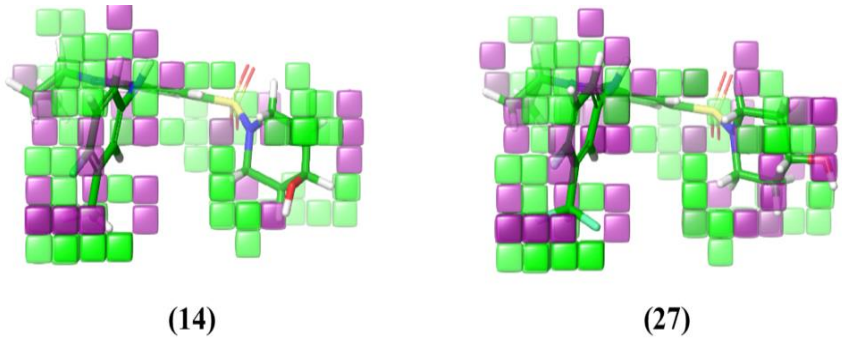

Fig. 3. Visualization of hydrophobic interaction from the 3D-QSAR model on the most active compound (14) and the least active compound (27).

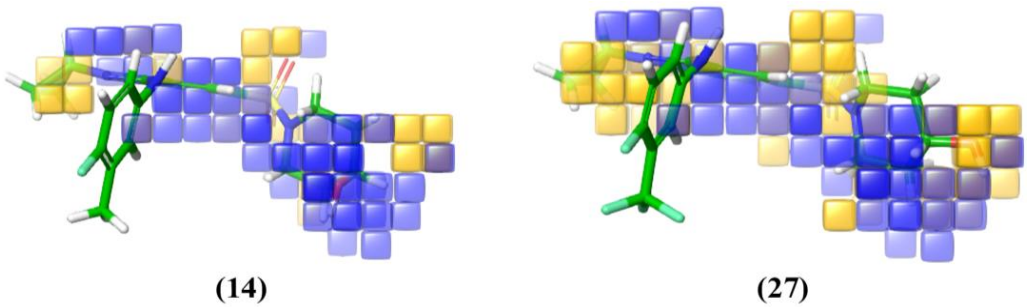

Fig. 4. Visualization of electron withdrawing from the 3D QSAR model on the most active compound (14) and the lowest active compound (27).

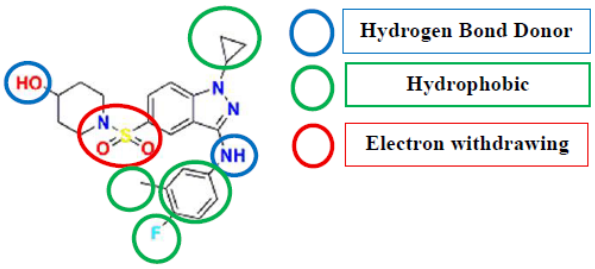

Fig. 5. Main structure-activity relationships derived from this study.

Docking Analysis of the Dataset

Molecular docking studies were performed to investigate the binding interactions of selected (1H-pyrazolo[3,4-c] pyridin-5-yl) sulfonamide derivatives with the hepatitis B virus (HBV) core protein (PDB ID: 5WRE). Two representative compounds, compounds 14 (the most active) and 27 (the least active), were evaluated and compared with two known HBV capsid assembly modulators, GLS4 and HAP-R01. The docking results are summarized in Table 4.

Compound 14 displayed the strongest binding affinity among the studied molecules, with an XP-Gscore of -8.812 kcal mol^{-1} and a Glide Emodel score of -93.765, indicating a highly stable interaction with the HBV core protein. Its binding mode is predominantly stabilized by hydrophobic interactions involving residues PHE110, TRP125, ILE105, and PHE122. In addition, it forms three key hydrogen bonds with SER141, SER121, and TRP102, with bond distances of 2.28 Å, 2.00 Å, and 2.06 Å, respectively. These interactions contribute significantly to the stable anchoring of the compound within the active site.

In contrast, compound 27 exhibits a significantly lower binding affinity, with an XP-Gscore of -5.702 kcal mol^{-1}, reflecting a reduced stabilization within the binding pocket. Although it shares similar hydrophobic contacts with PHE110, TRP125, ILE105, and PHE122, its hydrogen bond network is noticeably less favorable. The hydrogen bonds formed with SER141 (2.41 Å), SER121 (2.77 Å), and TRP102 (1.86 Å) include longer, less optimal distances, especially with SER121, which likely contribute to its diminished stabilization compared to compound 14.

The reference inhibitor GLS4 also demonstrated strong binding affinity, with an XP-Gscore of -8.738 kcal mol^{-1}. It formed key hydrogen bonds with TRP102 (1.95 A°) and SER106 (2.96 A°), along with a π-π stacking interaction with TYR118, which likely enhances its binding affinity. These interactions are comparable to those observed for compound 14, further supporting the promising activity of these analogs as HBV core protein inhibitors.

HAP-R01, a well-established HBV capsid assembly modulator, displayed the highest binding affinity among all tested compounds, with an XP-Gscore of -12.508 kcal mol^{-1} and the lowest Glide Emodel score of -103.420. It formed multiple hydrogen bonds with TRP102 (2.02 A°), SER106 (2.91 A°), SER141 (1.79 A°), and LEU140 (2.02 A°), and in addition to extensive hydrophobic and π–π stacking interactions with TYR118 (5.43 Å)**.** These results are consistent with its well-documented potent inhibitory activity. Figure 6 and Fig. 7 depict the two- and three-dimensional binding interactions of compounds 14, 27, GLS4, and HAP-R01 within the HBV core protein active site, illustrating their distinct interaction profiles.

Table 4. Docking Scores and Key Interactions of Ligands (14, 27, GLS4, HAP-R01) with HBV Core Protein (PDB ID: 5WRE)

Compd.	XP-Gscore	Glide emodel	Key interactions		
			H-Bonds	Hydrophobic	Pi-Pi
14	-8.812	-93.765	SER141(2.28A°), SER121(2.00A°), TRP102(2.06A°)	PHE110, TRO125, ILE105, PHE122	/
27	-5.702	-94.551	SER141(2.41A°), SER121(2.77A°), TRP102(1.86A°)	PHE110, TRO125, ILE105, PHE122	/
GLS4	-8.738	-91.787	SER106(2.69A°), TRP102(1.95A°)	PHE110, TRO125, ILE105, PHE122	TYR118(5.44A°)
HAP-R01	-12.508	-103.420	SER106(2.91A°), SER141(1.79A°), TRP102(2.02A°), LEU140(2.14A°)	PHE110, TRO125, ILE105, PHE122	TYR118(5.43A°)

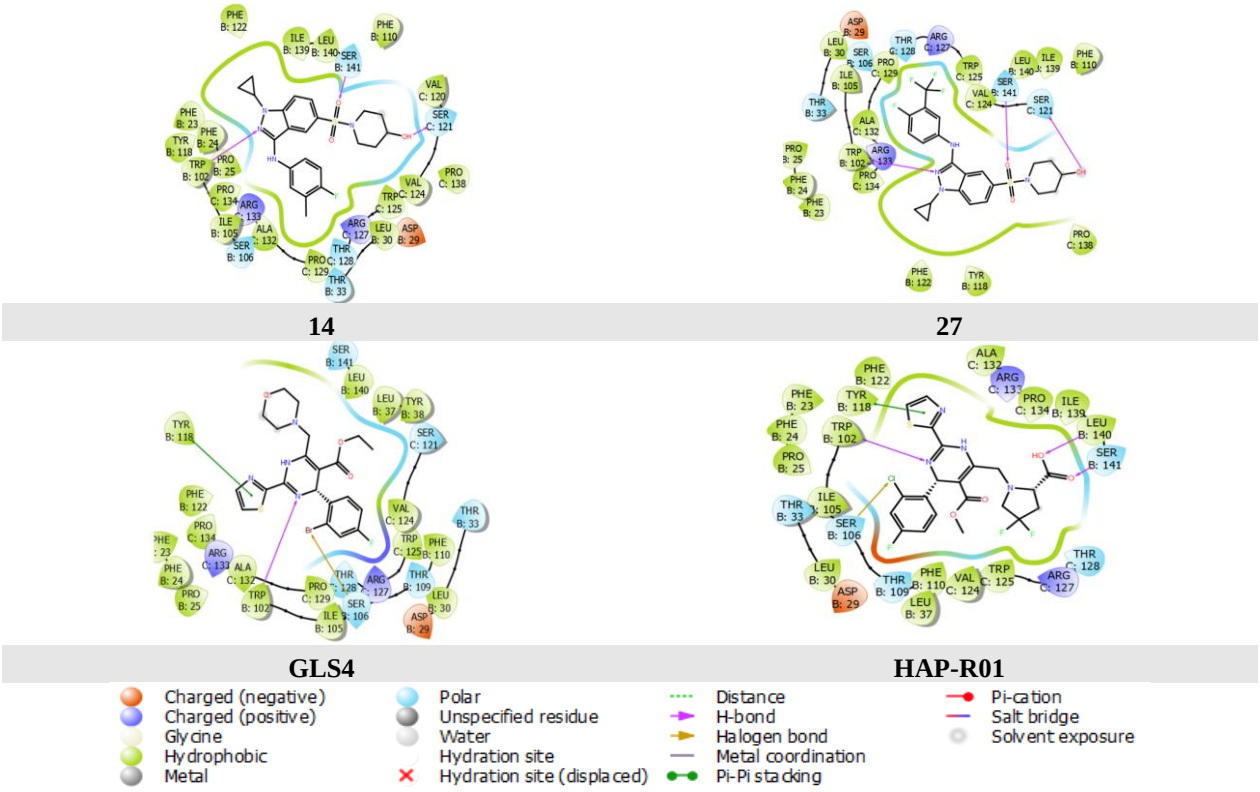

Fig. 6. Two-dimensional interaction diagrams of ligands 14, 27, GLS4, and HAP-R01 within the active site of the target protein (PDB ID: 5WRE).

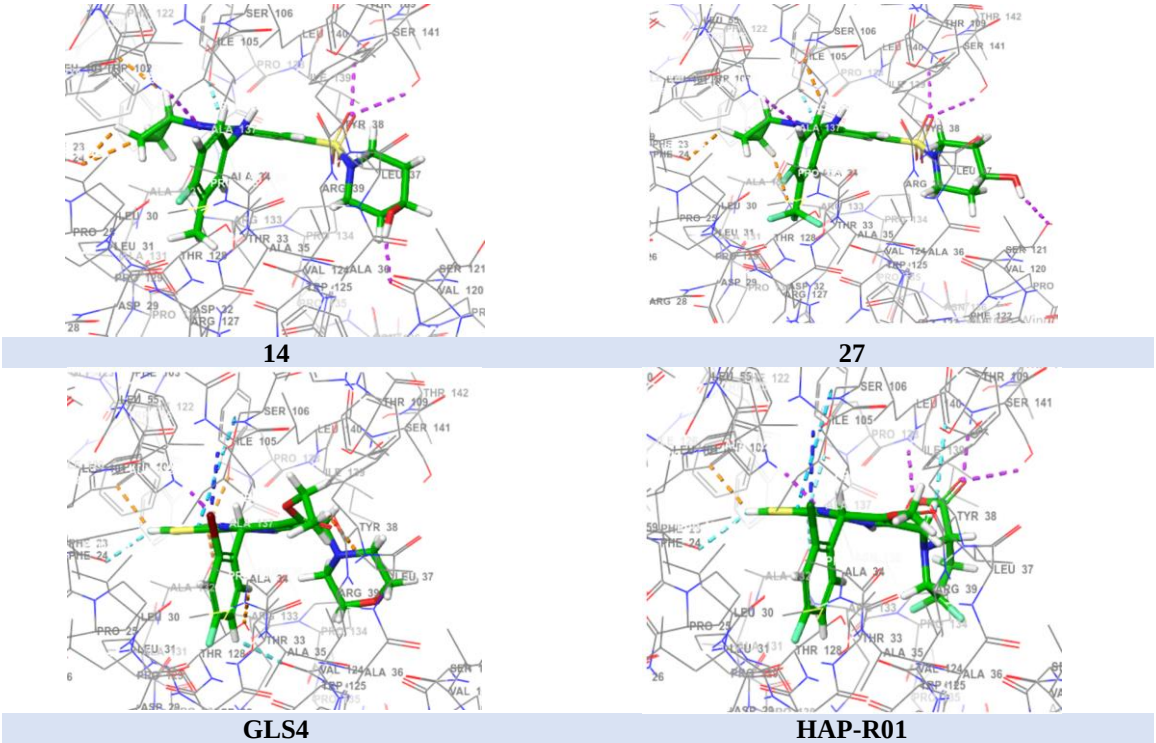

Fig. 7. Three-dimensional interaction diagrams of ligands 14, 27, GLS4, and HAP-R01 within the active site of the target protein (PDB ID: 5WRE).

Docking Validation Protocol

To assess its reliability, it is essential to perform redocking of co-crystal ligands before conducting molecular docking studies. Figure 8 shows highly superimposable and consistent conformations between the two poses, with an RMSD of 0.525 Å, less than 2 A°. This indicates that the docking protocol that was performed was reliable and could be used for subsequent studies.

Docking of Newly Designed Inhibitors

The newly designed compounds A1 to A5 (Fig. 9) were docked into the binding site of the HBV core protein (PDB ID: 5WRE) using Glide XP to evaluate their binding affinities and interaction profiles. The docking results are summarized in Table 5. Among these compounds, A1 exhibited the most favorable binding characteristics, with the lowest XP-Gscore of -9.047 kcal mol^{-1} and a strong Glide Emodel of -74.679, indicating a high affinity at the target site. A1 formed multiple hydrogen bonds (SER121, SER141, TRP102) and Pi-Pi (PHE23) stacking interactions comparable to those of standard reference inhibitors GLS4 and HAP-R01, indicating effective accommodation within the binding pocket. As for compound A2, the XP-Gscore value was -8.973 kcal mol^{-1}, while the lowest Glide Emodel score was -85.427, indicating excellent binding pose stability. It exhibited favorable interactions with key hydrogen bonds (SER121, SER141, SER106, TRP102) and hydrophobic interactions, and notably formed a stabilizing Pi-Pi interaction with residue PHE110, a feature often associated with potent inhibition. Compounds A3, A4, and A5 also showed consistent binding modes, with docking scores ranging from -8.636 to -8.226 kcal mol^{-1}. These compounds engaged in hydrogen bonding interactions (SER121, SER141, SER106, TRP102) and hydrophobic contacts, including important Pi-Pi interactions with aromatic residues such as PHE110 and TYR118.

Table 5. Docking Scores, Key Interactions of Newly Designed Inhibitors (A1-A5) with the HBV Core Protein (PDB ID: 5WRE) and Predicted Activity (PEC_{50})

Name	XP-	Glide	Key interactions			PEC_{50}
Compd	Gscore	emodel	H-Bonds	Hydrophobic	Pi-Pi	
A1	-9.047	-74.679	SER121 (1.75 A°), SER141(2.01 A°), TRP102(2.37A°)	ILE105, TRP102, PRO138, PHE122, TRP125, ILE139	PHE23 (4.35A°)	7.282
A2	-8.973	-85.427	SER121(1.79A°), SER141(2.42A°), SER106(2.61A°), THR128(1.91A°)	LEU140, ILE105, TRP102, PRO138, PHE122, TRP125	PHE110(4.70A°)	6.742
A3	-8.636	-73.389	SER121(1.78A°), SER141(2.39A°), SER106(2.67A°), THR128(2.27A°)	ILE105, TRP102, PRO138, PHE122, TRP125, ILE139	PHE110(4.76A°)	6.720
A4	-8.371	-69.901	SER121(1.95A°), SER141(2.31A°), SER106(3.15A°), LEU140(2.00A°).	PHE110, TRP125, TRP102 ILE105, PHE122	PHE110 (5.28A°,4.93A°)	6.798
A5	-8.226	-80.026	SER121(2.24A°), SER141(2.38A°)	LEU140, PHE110, PRO134, TRP125, ILE105, PHE122	TYP118(5.33A°)	6.502

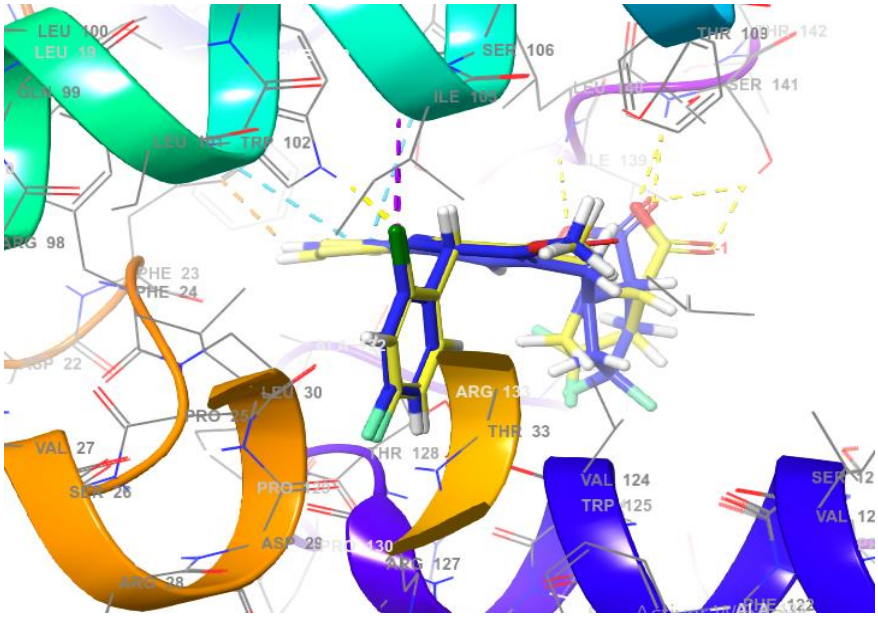

Fig. 8. Superimposed binding modes of X-ray–bound HAP-R01 (yellow) and redocked HAP-R01 (blue) in complex with 5WRE.

Table 6. Predicted ADME Properties of Newly Designed and Reference Compounds

Compounds name	MW (≤ 500)	SASA (300–1000)	HBA	HBD	Qplog Po/w (-2 to 6.5)	QPlogS (-6.5 to 0.5)	QPlogKhsa	QPPMDCK (< 25 poor,>500 good)	QPP Caco-2	Qplog BB (-3.0 to 1.2)	QPlogPoct	QPlogPW (4 to 45)	%HOA (20-80%)	PSA (≤ 140 Å²)
A1	477.57	770.96	10.2	3.0	3.00	-6.13	0.17	379.85	292.2	-1.28	26.46	17.45	88.66	112.3
A2	548.42	768.75	11.7	3.0	2.19	-4.76	-0.19	396.83	73.64	-0.69	27.03	18.84	60.28	109.6
A3	544.46	791.51	11.7	3.0	2.20	-4.89	-0.11	193.73	68.48	-0.89	27.27	18.80	59.70	109.4
A4	479.96	778.51	10.2	3.0	2.51	-4.94	0.09	109.49	69.16	-0.98	26.22	17.60	74.59	107.2
A5	445.51	756.87	10.2	3.0	2.06	-4.32	-0.01	49.455	68.86	-1.11	25.48	17.08	71.88	107.3
14	444.52	700.07	7.0	2.0	3.49	-5.56	0.41	360.32	472.8	-1.02	22.43	13.09	95.23	88.46
GLS4	509.39	721.16	7.7	0.0	4.10	-4.60	0.24	2489.3	776.2	0.53	20.01	10.036	89.71	74.45
HAP-R01	514.91	714.02	8.0	1.0	2.75	-5.96	0.35	407.60	56.77	0.14	23.03	12.18	61.49	110.51

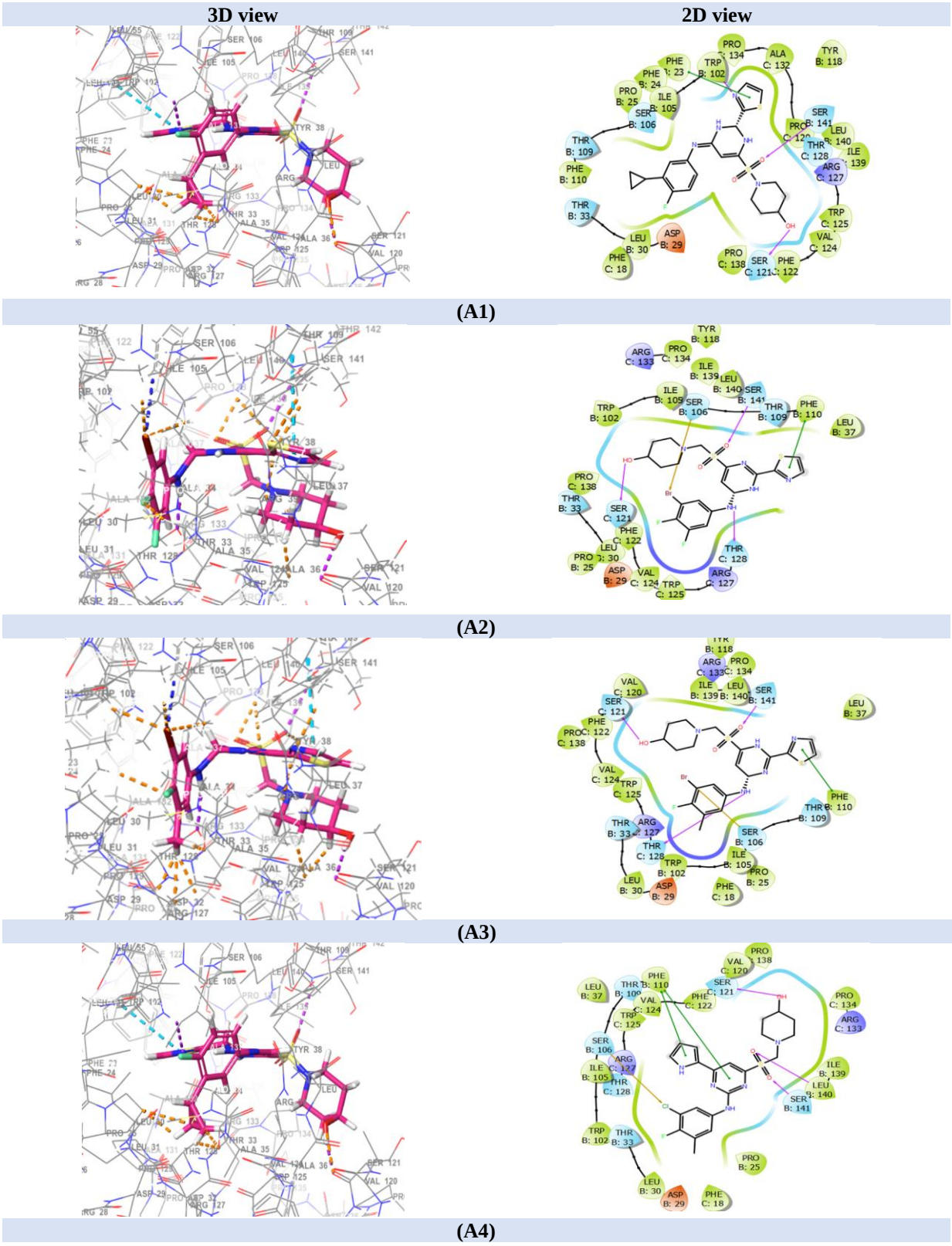

Fig. 9. 2D and 3D Interaction Diagrams of Designed Inhibitors A1-A5 with HBV Core Protein Binding Site.

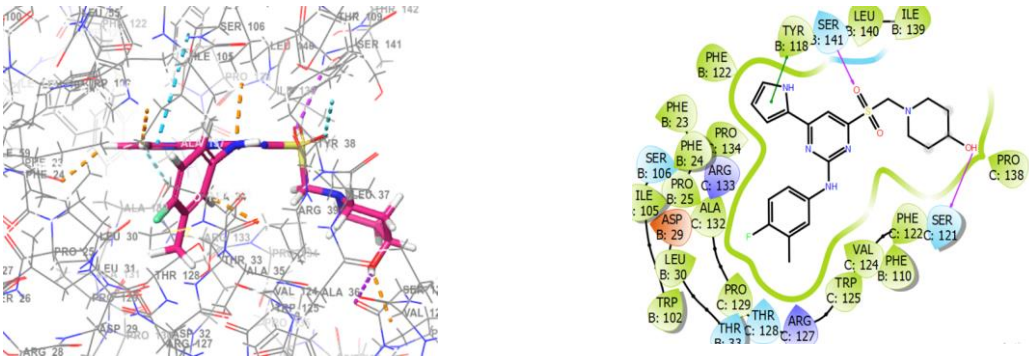

(A5)

Fig. 9. 2D and 3D Interaction Diagrams of Designed Inhibitors A1-A5 with HBV Core Protein Binding Site.

ADME Predictions of Newly Designed Compounds

The predicted ADME profiles of the newly designed compounds A1–A5 indicate overall drug-like properties, but a closer examination highlights both strengths and potential liabilities. All compounds have molecular weights within an acceptable range (445-548 Da) and favorable polar surface areas (107-112 Å²), supporting oral bioavailability. Predicted lipophilicity (QPlogPo/w: 2.06-3.00) and aqueous solubility (QPlogS: -6.13 to -4.32) suggest a reasonable balance between membrane permeability and solubility. However, some limitations were observed. Compounds A2-A5 display moderate Caco-2 permeability, which may restrict intestinal absorption compared to A1, potentially reducing systemic exposure. Additionally, PSA values at the higher end (~112 Å²) could negatively affect passive membrane diffusion. Brain-blood partition coefficients (QlogBB: -1.28 to -0.69) indicate limited CNS penetration, which is favorable for avoiding central side effects but may be a liability if CNS activity were desired. Overall, while minor limitations exist, all compounds remain within acceptable ranges for drug-like properties. These findings support the potential of A1–A5 as promising candidates for further development as HBV capsid assembly modulators.

CONCLUSION

In this study, a comprehensive computational approach was applied to investigate (1H-Pyrazolo[3,4-c] pyridin-5-yl) sulfonamide derivatives as potential hepatitis B virus (HBV) capsid assembly modulators. The atom-based 3D-QSAR model demonstrated strong statistical robustness and excellent predictive capability (R^2 = 0.97, Q^2 = 0.80, RMSE = 0.17), highlighting the pivotal roles of hydrophobic interactions, electron-withdrawing groups, and hydrogen bond donors in modulating biological activity. Molecular docking studies revealed favorable binding affinities and key interactions of both reported and newly designed compounds within the HBV core protein active site. Importantly, the newly designed inhibitors demonstrated promising docking scores and interaction profiles comparable to known reference inhibitors GLS4 and HAP-R01. ADME predictions further supported the drug-like properties of these compounds, indicating good pharmacokinetic profiles and potential for oral bioavailability.

REFERENCES

[1] Hu, Y.; Zhang, Y.; Jiang, W., Targeting hepatitis B virus-associated nephropathy: efficacy and challenges of current antiviral treatments. *Clin. Exp. Med.* **2025**, *25*, 57. DOI: 10.1007/s10238-025-01584-4.

[2] Marjenberg, Z.; Wright, C.; Pooley, N.; *et al*., Hepatitis B surface antigen prevalence and the rates of mother-to-child transmission of hepatitis B virus after the introduction of infant vaccination programs in South East Asia and Western Pacific regions: a systematic review. *Int. J. Infect. Dis.* **2022**, *124*, 65-75. DOI: 10.1016/j.ijid.2022.09.003.

[3] Abdelhamed, W.; El-Kassas, M., Hepatitis B virus as a risk factor for hepatocellular carcinoma: There is still

much work to do. *Liver. Res.* **2024**, *8*, 83-90. DOI: 10.1016/j.livres.2024.05.004.

[4] Broquetas, T.; Carrión, J. A., Current Perspectives on Nucleos(t)ide Analogue Therapy for the Long-Term Treatment of Hepatitis B Virus. *Hepat. Med.* **2022**, *14*, 87-100. DOI:10.2147/HMER.S291976.

[5] Ren, J.; Cheng, S.; Ren, F.; *et al*., Epigenetic regulation and its therapeutic potential in hepatitis B virus covalently closed circular DNA. *Genes. Dis.* **2025**, *12*, *1*, 101215. DOI: 10.1016/j.gendis.2024.101215.

[6] Wang, Z.; Wang, W.; Wang, L., Epigenetic regulation of covalently closed circular DNA minichromosome in hepatitis B virus infection. *Biophys. Rep.* **2020**, *6*, 115-126. DOI: 10.1007/s41048-020-00112-z.

[7] Gómez-Moreno, A.; Ploss, A., Mechanisms of Hepatitis B Virus cccDNA and Minichromosome Formation and HBV Gene Transcription. *Viruses.* **2024**, *16, 4*, 609. DOI: 10.3390/v16040609.

[8] Viswanathan, U.; Mani, N.; Hu, Z.; *et al*., Targeting the multifunctional HBV core protein as a potential cure for chronic hepatitis B. *Antiviral. Res.* **2020**, *182*, 104917. DOI: 10.1016/j.antiviral.2020.104917.

[9] Qazi, S.; Schlicksup, C. J.; Rittichier, J.; *et al*., An Assembly-Activating Site in the Hepatitis B Virus Capsid Protein Can Also Trigger Disassembly. *ACS. Chem. Biol*. **2018**, *13*, 2114-2120. DOI: 10.1021/acschembio.8b00283.

[10] Tolufashe, G.; Viswanathan, U.; Kulp, J.; Guo, J. T., Computational Approaches to Predict Hepatitis B Virus Capsid Protein Mutations That Confer Resistance to Capsid Assembly Modulators. *Viruses.* **2025**, *17*, *3*, 332. DOI: 10.3390/v17030332.

[11] Wang, C.; Pei, Y.; Pei, Y.; *et al*., Discovery of (1H-Pyrazolo [3,4-c] pyridin-5-yl) sulfonamide Analogues as Hepatitis B Virus Capsid Assembly Modulators by Conformation Constraint. *J. Med. Chem*. **2020**, *63*, 6066-6089. DOI: 10.1021/acs.jmedchem.0c00292.

[12] Shah, M.; Patel, M.; Shah, M.; *et al*., Computational transformation in drug discovery: A comprehensive study on molecular docking and quantitative structure activity relationship (QSAR). *Intelligent Pharmacy*. **2024**, *2*, 589-595. DOI: 10.1016/j.ipha.2024.03.001.

[13] Güzel, Y.; Karakaya, S.; Wang, L.; *et al*., 3D-QSAR modeling with selection of local reactive descriptors (LRD) and molecular docking studies on diarylpyrazole-benzenesulfonamide derivatives. *Comput. Biol. Chem*. **2025**, *118*, 108489. DOI: 0.1016/ j.compbiolchem.2025.108489.

[14] Moussaoui, M.; Baammi, S.; Soufi, H.; *et al*., QSAR, ADMET, molecular docking, and dynamics studies of 1,2,4-triazine-3(2H)-one derivatives as tubulin inhibitors for breast cancer therapy. *Sci. Rep*. **2024**, *14*. DOI: 10.1038/s41598-024-66877-2.

[15] Kaur, N.; Gupta, S.; Pal, J.; *et al*., Design of BBB permeable BACE-1 inhibitor as potential drug candidate for Alzheimer disease: 2D-QSAR, molecular docking, ADMET, molecular dynamics, MMGBSA. *Comput. Biol. Chem*. **2025**, *116*, 108371. DOI: 10.1016/ j.compbiolchem.2025.108371.

[16] Trezza, A.; Visibelli, A.; Roncaglia, B.; *et al*., Unveiling Dynamic Hotspots in Protein-Ligand Binding: Accelerating Target and Drug Discovery Approaches. *Int. J. Mol. Sci.* **2025**, *26*. DOI: 10.3390/ijms26093971.

[17] Alici, H., Structure-Based Design and *In-Silico* Evaluation of Computationally Proposed Curcumin Derivatives as Potential Inhibitors of the Coronaviral PLpro Enzymes. *Pharmaceuticals*. **2025**, *18*. DOI: 10.3390/ph18060798.

[18] Huggins, D. J.; Sherman, W.; Tidor, B., Rational approaches to improving selectivity in drug design. *J. Med. Chem*. **2012**, *55*, 1424-1444. DOI: 10.1021/ jm2010332.

[19] Laoud, A.; Belafriekh, A.; Alaqarbeh, M., N-Phenyl-3-sulfamoyl-benzamide derivatives as anti-hepatitis B virus agent candidates. Integrated computational studies. *J. Serb. Chem. Soc.*, **2025**, *10*, 1175-1187. DOI: 10.2298/JSC250430060L.

[20] Laoud, A.; Ali-Rachedi, F.; Ferkous, F., Discovery of New Inhibitors of Enoyl-ACP Reductase *via* Structure-Based Virtual Screening. *Phys. Chem. Res*. **2023**, *11*, 459-469. DOI: 10.22036/ pcr.2022.342259.2106.

[21] Panigrahi, D.; Sahu, S. K., Computational approaches: atom-based 3D-QSAR, molecular docking, ADME-Tox, MD simulation and DFT to find novel multi-targeted anti-tubercular agents. *BMC. Chem*. **2025**, *19*, 39. DOI: 10.1186/s13065-024-01357-2.

[22] Kushavah, U.; Mahapatra, P. P.; Ahmed, S.; Siddiqi, M. I., Pharmacophore-based 3D-QSAR modeling, virtual screening, docking, molecular dynamics and biological evaluation studies for identification of potential inhibitors of alpha-glucosidase. *J. Mol. Model*. **2024**, *30*, 389. DOI: 10.1007/s00894-024-06181-y.

[23] Zhou, Z.; Hu, T.; Zhou, X.; *et al*., Heteroaryldihydropyrimidine (HAP) and Sulfamoylbenzamide (SBA) Inhibit Hepatitis B Virus Replication by Different Molecular Mechanisms. *Sci. Rep*. **2017**, *7*, 42374. DOI:10.1038/srep42374.

[24] Belafriekh, A.; Laoud, A.; Elmchichi, E.; Bouachrine, M., *In Silico* Approach for Developing New Anti-Tuberculosis Drug Candidates: 3D-QSAR, Molecular Docking and ADME Studies of Pretomanid Derivatives. *Phys. Chem. Res.* **2024**, *12*, 729-743. DOI: 10.22036/pcr.2024.425052.2448.

[25] Ajjarapu, S. M.; Tiwari, A.; Taj, G.; *et al*., Simulation studies, 3D QSAR and molecular docking on a point mutation of protein kinase B with flavonoids targeting ovarian Cancer. *BMC. Pharmacol. Toxicol.* **2021**, *22*. DOI: 10.1186/s40360-021-00512-y.

[26] Laoud, A.; Ferkous, F.; Maccari, L.; *et al*., Identification of novel nt-MGAM inhibitors for potential treatment of type 2 diabetes: Virtual screening, atom-based 3D-QSAR model, docking analysis and ADME study. *Comput. Biol. Chem*. **2018**, *72*, 122-135. DOI: 10.1016/j.compbiolchem.2017.12.003.

[27] Panwar, U.; Singh, S. K., Atom-based 3D-QSAR, molecular docking, DFT, and simulation studies of acylhydrazone, hydrazine, and diazene derivatives as IN-LEDGF/p75 inhibitors. *Struct. Chem*. **2021**, *32*, 337-352. DOI: 10.1007/s11224-020-01628-3.

[28] Tabti, K.; Sbai, A.; Maghat, H.; *et al*., Discovery of novel indoleamine 2,3-dioxygenase-1 (IDO-1) inhibitors: pharmacophore-based 3D-QSAR, Gaussian field-based 3D-QSAR, docking, and binding free energy studies. *Struct. Chem*. **2024**, *35*, 135-160. DOI: 10.1007/s11224-023-02213-0.

[29] Teli, M. K.; Rajanikant, R. G., Pharmacophore generation and atom-based 3D-QSAR of N-iso-propyl pyrrole-based derivatives as HMG-CoA reductase inhibitors. *Org. Med. Chem. Lett.*, **2012**, *2*, 25. DOI: 10.1186/2191-2858-2-25.

[30] Asgaonkar, K. D.; Patil, S. M.; Chitre, T. S.; *et al*., Use of Pharmacophore Modeling, 3D-atom-based QSAR, ADMET, Docking, and Molecular Dynamics Studies for the Development of Psoralen-based Derivatives as Antifungal Agents. *Anti-infect. Agents*. **2024**, *22*, *3*, 33-47. DOI: 10.2174/0122113525279683231228130206.

[31] Khaldan, A.; Bouamrane, S.; Ouabane, M.; *et al*., Design, 3D-QSAR, molecular docking, MD simulations, ADME/Tox properties and DFT study of benzimidazole derivatives as promising α-glucosidase inhibitors. *J. Mol. Struct*. **2025**, 1328. DOI: 10.1016/j.molstruc.2025.141351.

[32] Parmar, M. P.; Das, A.; Vala, D. P.; *et al*., QSAR, Antimicrobial, and Antiproliferative Study of (R/S)-2-Thioxo-3,4-dihydropyrimidine-5-carboxanilides. *ACS. Omega*. **2025**, *10*, 7013-7026. DOI: 10.1021/acsomega.4c09899.

[33] Lanka, G.; Banerjee, S.; Adhikari, N.; Ghosh, B., Fragment-based discovery of new potential DNMT1 inhibitors integrating multiple pharmacophore modeling, 3D-QSAR, virtual screening, molecular docking, ADME, and molecular dynamics simulation approaches. *Mol. Divers*. **2025**, *29*, 117-137. DOI: 10.1007/s11030-024-10837-5.